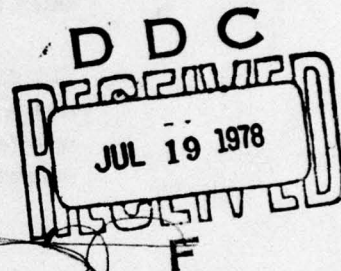LEVEL Ⅱ (13)

AD A056582

ESR CENTERS AND CHARGE DEFECTS NEAR THE SILICON/ SILICON DIOXIDE INTERFACE

D D C
JUL 19 1978
F

Edward H. Poindexter
Edwin R. Ahlstrom
Philip J. Caplan

Electronics Technology & Devices Laboratory

April 1978

ERADCOM

US ARMY ELECTRONICS RESEARCH & DEVELOPMENT COMMAND
FORT MONMOUTH, NEW JERSEY 07703

78 07 10 118

AD No.
DDC FILE COPY

NOTICES

Disclaimers

The findings in this report are not to be construed as an official Department of the Army position, unless so designated by other authorized documents.

The citation of trade names and names of manufacturers in this report is not to be construed as official Government indorsement or approval of commercial products or services referenced herein.

Disposition

Destroy this report when it is no longer needed. Do not return it to the originator.

REPORT DOCUMENTATION PAGE

READ INSTRUCTIONS BEFORE COMPLETING FORM

1. REPORT NUMBER	2. GOVT ACCESSION NO.	3. RECIPIENT'S CATALOG NUMBER
DELET-TR-78-9		

4. TITLE (and Subtitle)
ESR CENTERS AND CHARGE DEFECTS NEAR THE SILICON/SILICON DIOXIDE INTERFACE.

5. TYPE OF REPORT & PERIOD COVERED

6. PERFORMING ORG. REPORT NUMBER

7. AUTHOR(s)
Edward H. Poindexter
Edwin R. Ahlstrom
Philip J. Caplan

8. CONTRACT OR GRANT NUMBER(s)
C7

9. PERFORMING ORGANIZATION NAME AND ADDRESS
Electronic Materials Research Division
US Army Electronics Technology & Devices Laboratory
(ERADCOM), Fort Monmouth, NJ 07703 DELET-ED

10. PROGRAM ELEMENT, PROJECT, TASK AREA & WORK UNIT NUMBERS
61102A
1L161102AH47 C7 021

11. CONTROLLING OFFICE NAME AND ADDRESS
US Army Electronics Research & Development Command
Fort Monmouth, NJ 07703
DELET-ED

12. REPORT DATE
April 1978

13. NUMBER OF PAGES
5

14. MONITORING AGENCY NAME & ADDRESS(if different from Controlling Office)

15. SECURITY CLASS. (of this report)
Unclassified

15a. DECLASSIFICATION/DOWNGRADING SCHEDULE

16. DISTRIBUTION STATEMENT (of this Report)

Approved for public release; distribution unlimited.

17. DISTRIBUTION STATEMENT (of the abstract entered in Block 20, if different from Report)

18. SUPPLEMENTARY NOTES
Paper was presented at the International Topical Conference on the Physics of SiO_2 and Its Interfaces, Yorktown Heights, N.Y., 22-24 March 1978. To be published in the Proceedings.

19. KEY WORDS (Continue on reverse side if necessary and identify by block number)
Silicon dioxide
Semiconductor interfaces
Surface states
MOS structures

20. ABSTRACT (Continue on reverse side if necessary and identify by block number)
The Nishi-B esr center has been examined as a function of thermal oxidation and annealing conditions in single-crystal silicon wafers. It was observed that B concentration was not correlated with fixed surface-state charge density Q, despite some similarities in their behavior. In freshly oxidized wafers, B typically ranges up to 200 per nm sq, and Q up to 50 per nm sq. The concentration of B is highly dependent on cooling rates; concentration does not depend on oxide thickness and B may be observed even in native oxides. The g-value of the orientation-averaged B signal (2.0064) favors its assignment to trivalent Si →

next page

DD FORM 1473 EDITION OF 1 NOV 65 IS OBSOLETE

UNCLASSIFIED

20. Abstract (cont'd)

in a silicon environment, as in crushed silicon (2.0055), rather than to the well-studied E centers (2.0008) found in various forms of damaged silicon dioxide. In our thermal oxides, E centers were unobservable, and thus cannot be the main source of Q, despite their nominal positive charge. Preliminary evidence shows a correlation of B with initial, unannealed "fast" interface states N, supporting the idea that trivalent Si is the origin of these states.

CONTENTS

FIGURES

TABLES

ESR CENTERS AND CHARGE DEFECTS NEAR THE Si/SiO$_2$ INTERFACE

Edward H. Poindexter, Edwin R. Ahlstrom, and Philip J. Caplan
US Army Electronics Technology and Devices Laboratory (ERADCOM)
Fort Monmouth, N.J. 07703

ABSTRACT

The esr center P_b has been examined as a function of thermal oxidation and annealing conditions in single-crystal silicon wafers. It was observed that P_b concentration was not correlated with fixed surface-state charge density Q_{ss}, despite some similarities in their behavior. In freshly oxidized wafers, P_b typically ranges up to 2×10^{12} cm^{-2}, and Q_{ss} up to 5×10^{11} cm^{-2}. The concentration of P_b is highly dependent on cooling rates; concentration does not depend on oxide thickness and P_b may be observed even in native oxides. The g-value of the orientation-averaged P_b signal (2.0064) favors its assignment to Si^{III} in a silicon environment, as in crushed silicon (2.0055), rather than to the well-studied E' centers (2.0008) found in various forms of damaged SiO$_2$. In our thermal oxides, E' centers were unobservable, and thus cannot be the main source of Q_{ss}, despite their nominal positive charge. Preliminary evidence shows a correlation of P_b with initial, unannealed "fast" interface states N_{st}, supporting the idea that Si^{III} is the origin of these states.

INTRODUCTION

High-performance integrated circuit devices are required for a variety of advanced military electronic systems. The performance and reliability of these devices can be unacceptably degraded by the presence of certain atomic-scale defects near the Si/SiO$_2$ interface, which can cause noise, loss of gain, bias drifts, and ultimate failure. Diagnosis and control of these defects is essential as IC devices move into the submicron regime.

Extensive studies of the Si/SiO$_2$ interface by electrical methods have not defined the origins of interface defects (1). The wealth of esr studies of silicon, quartz, and glass suggests application of esr to the interface. Nishi (2) observed and tentatively identified three main esr signals from thermally oxidized silicon wafers, P_a, P_b, P_c. The P_b signal, visible at 300 K (3), seems to have the greatest significance for the defect structure of the Si/SiO$_2$ interface. Our study was prompted by Nishi's tentative identification of P_b with the E' centers of damaged silica, and by the implied connection between P_b and surface charge Q_{ss} evidenced by similar depth profiles. We have attempted to confirm these conclusions or offer alternatives.

EXPERIMENTAL DETAILS

The samples were from n- and p-type Monsanto double-polished wafers, 100-300 ohm-cm. They were cleaned and oxidized in a quartz-tube diffusion furnace by standard semiconductor procedures. For C-V measurements, one-micron aluminum was evaporated onto the etched or sandblasted back surface and 1.2 mm dots were evaporated onto the oxide. A PAR system was used at 1.0 MHz. Samples consisted of 4 to 6 pieces 4x20 mm, with [111] or [100] face. A Varian 4501 with dual cavity was used for spin concentration, and an E-line Century for anisotropy and line structure. An H-P 5480 signal averager was used. All runs were at 300 K.

1

RESULTS AND DISCUSSION

Character of Esr Signals

Samples with [111] face showed P_b signals (P_b[111]) with up to 20:1 signal-noise without averaging. A typical P_b[111] signal is shown in Fig. 1a. The line shows reproducible structure which is symmetrical about the center, and is superimposed on a wider low-amplitude signal which contributes to an anisotropic asymmetry of the line base. This latter signal is mostly residual silicon damage at g=2.0055. In Fig. 1b, the signal has been accumulated 400 times; much detail is seen, nearly all from the silicon. Hoped-for symmetrical hyperfine lines are not evident in the clutter, with the possible exception of the close-in blips noted above.
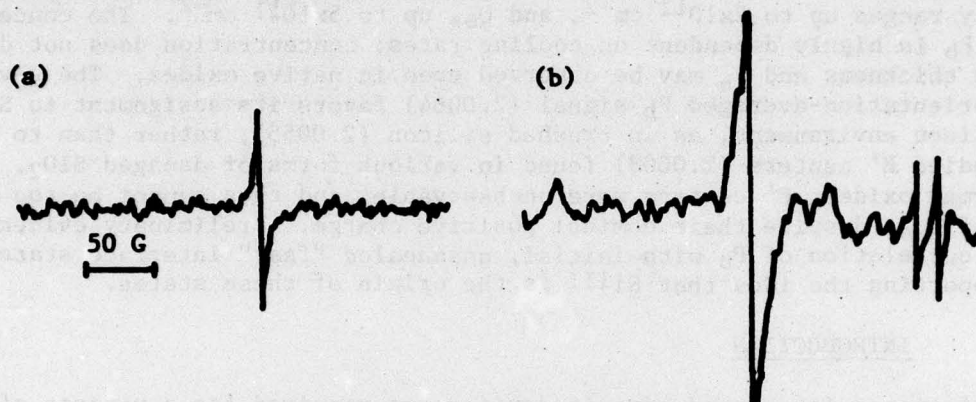

Fig. 1. P_b signal from [111] silicon (a) one trace (b) 400 traces.

Signals from the [100] face are different (Fig. 2). The s-n ratio is much worse than P_b[111] signals; 16 to 64 traces were used. The line has several ill-defined components, with narrowest, least-structured appearance at ~ 25°-30° from [100] face axis. Resolution is impossible at this time.

Fig. 2. P_b signal from [100] silicon (a) $H_o \perp$[100] face (b) $H_o \perp$[110].

Anisotropy of P_b[111] (2) is well confirmed in our studies. Within errors, our signal shows [111] axial symmetry, $g_{\parallel}$ =2.0013, $g_{\perp}$ =2.0081. The g-map is shown in Fig. 3. Only one limb is observed, for spin centers with major axis normal to the interface. The line width of P_b[111] varies from 1 G on [111] to 3 G at 90°. For P_b[100] (not shown) one possible but arbitrary deconvolution gives 2 components with g-anisotropy like P_b[111].

Identification of Centers

The anisotropy and g-values of P_b[111] are like other centers observed in

2

$[100]$ $[111]$ $[110]$ $[11\bar{2}]$ $[\bar{1}00]$ (a)

$[111]$ $[1\bar{1}0]$ (b)
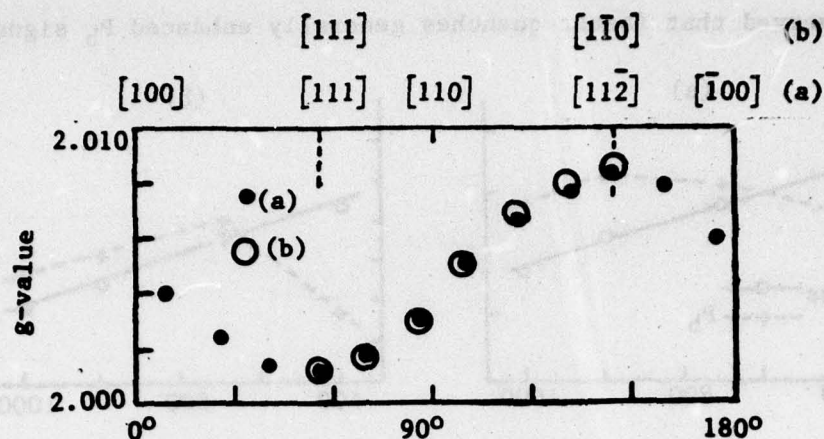
g-value: 2.010 ... 2.000

0°   90°   180°

Fig. 3. g-anisotropy for P_b $[111]$, rotation plane (a) $[11\bar{2}]$ (b) $[1\bar{1}0]$.

irradiated silicon (4-6) which have been ascribed to Si^{III} with unbonded orbital facing into a vacancy. In a study of the Si-E center (vacancy plus phosphorus), Watkins and Corbett (5) calculate the anisotropy for a Si^{III} fragment ($\Delta g_{\parallel} \sim 0$; $\Delta g_{\perp} \sim +0.017$). They ascribe the deficiency vis-a-vis observed values ($g_1 = 2.0005$, $g_2 = 2.0112$, $g_3 = 2.0096$) to delocalization, and the hfs is consistent. Other well-characterized centers having similar anisotropy are the negatively-charged divacancy (G-7) (6), and the low-temperature form of the five-vacancy cluster (4). In view of the similarity of $P_b [111]$ to these Si^{III} defects, we assign it to Si^{III} bonded to silicon, not oxygen, with unpaired p-rich orbital normal to the interface. The variation in line width may reflect different g-values in different sites.

$P_b [111]$ is not like the E' center of damaged quartz (7 - 8), which has a lower g_{av} and much weaker, prolate anisotropy ($g_1 = 2.0018$, $g_2 = 2.0005$, $g_3 = 2.0003$).

The identification of $P_b [100]$ is not clear at present. We have been unable to resolve its map into combinations of single Si^{III} signals or bent-bond signals (like the Si-B1 center, structurally plausible for the $[100]$ face).

Relation to Interface Charge Defects

It is well known that Q_{ss} in thermal oxides is controlled by the final annealing temperatures (Deal triangle) (1). Figure 4 shows a series of p- and n-type samples grown at 1000 C in dry O_2, but annealed for an hour in O_2 at various temperatures. For both p and n, Q_{ss} values were found to follow the trend of the Deal triangle; the magnitude of $P_b [111]$ did not. This is contrary to our first tests, where correlation existed between P_b and Q_{ss} (9). (Earlier samples were erratically cooled.)

The values of Q_{ss} increase with longer cooling time (1). Table I shows the variation of $P_b [111]$ with cooling rate. After oxide growth, one sample was given the standard fast pull, and the other was cooled slowly in situ by turning off the furnace, while the oxygen continued to flow. Also compared are two samples annealed one hour in N_2 after oxidation, and respectively slow- and fast-cooled in N_2. The P_b results are different from Q_{ss}. The sample slow-cooled in O_2 had Q_{ss} about three times higher than the other samples, as expected. But the P_b signal is lower in the slow-cooled samples, whether the oxidation is followed by a nitrogen anneal or not. Nishi (2)

3

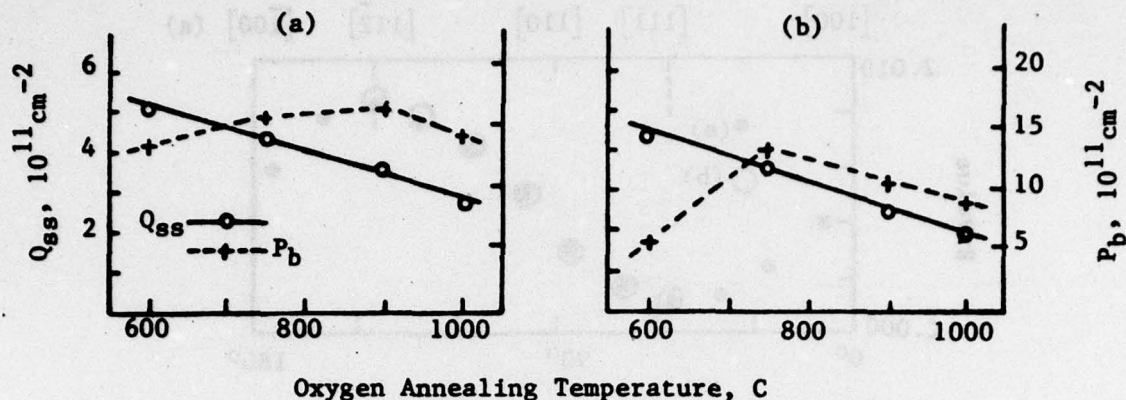likewise observed that faster quenches generally enhanced P_b signals.

Fig. 4. P_b signal vs Q_{ss} on [111] (a) p-Si (b) n-Si.

The dependence of P_b[111] centers on grown-oxide thickness reflects their
site and origin. The spin concentrations shown in Table II are constant over
two orders of magnitude in thickness. Moreover, we have recently observed P_b
with nitrogen-annealed native oxides. Our results disagree with Nishi's re-
port (2) of large increase in P_b from 2000 Å to 4000 Å, and are inconsistent
with the depth profile obtained by etching (2), which peaks at $\geq$ 150 Å. Con-
stant P_b suggests association with the immediate interface region only.

A seemingly oxide-located signal might come from small islands of silicon in
the oxide or from centers in the silicon surface whose paramagnetism disap-
pears when the last remnants of the oxide overburden are removed. A stress-
related center would behave in the latter fashion (10). Si^{III} with unpaired
orbital directed perpendicular to the interface is much more reasonable chem-
ically than preferential Si^{III} orientation far out in the oxide. In this
view, neither P_b centers nor unobserved E' centers are the major source of
Q_{ss}. (Quasi-E' centers--a doubly-charged pair of Si^{III}, or isolated singly-
charged Si, invisible to esr--are not ruled out.)

Table I. P_b vs cooling rate.			Table II. P_b vs oxide thickness.	
Cooling Conditions	Q_{ss} (Rel.)	Spin Conc. (Rel.)	Oxide Thickness (Å)	Spin Conc. (Rel.)
O_2 fast cool	3.5	3.4	100	2.9
O_2 slow cool	11.	1.5	300	3.2
N_2 fast cool	3.5	3.6	530	3.7
N_2 slow cool	3.5	0.6	1,560	3.7
			3,400	4.3
			12,760	3.7

Lack of correlation of P_b and Q_{ss} must be viewed in respect to usual device
processing regimens. Determination of Q_{ss} is assumed to be made after alu-
minum dot deposition and annealing--this reduces N_{st} (1) and allows a tract-
able C-V plot of the presumably unaffected fixed charge. The concentration
of interface states N_{st} in freshly oxidized wafers is of the same order as

4

P_b, 10^{12} cm^{-2}. Esr spectra, however, are taken on wafers which have not been "alnealed." We prepared a sample with substantial P_b signal, deposited aluminum over the sample surface, and "alnealed" it. After removing the aluminum, there was no detectable esr. Nishi (2) has noted that water vapor during oxidation affects P_b and N_{st} similarly. Finally, weaker P_b signals on [100] faces correlate with lower N_{st} values typical of [100] wafers.

In summary, we believe that the P_b[111] signal arises from Si^{III} at the interface, and that it is not the source of Q_{ss}. Furthermore, silica E' centers, not observed by esr in oxidized wafers, are likewise not a major source of Q_{ss}. Presently, the observed evidence favors a closer relation between P_b and N_{st} than between P_b and Q_{ss}. If substantiated, this would help to confirm the concept that Si^{III} is a source of initial interface states.

REFERENCES

1. B.E. Deal, The current understanding of charges in the thermally oxidized silicon structure, J. Electrochem. Soc. 121, 198C (1974).

2. Y. Nishi, Study of silicon-silicon dioxide structure by electron spin resonance I, Japan J. Appl. Phys. 10, 51 (1971).

3. P.J. Caplan, J.N. Helbert, B.E. Wagner, and E.H. Poindexter, Paramagnetic defects in silicon/silicon dioxide systems, Surface Science 54, 33 (1976).

4. Y.-H. Lee and J.W. Corbett, EPR studies in neutron-irradiated silicon: a negative charge state of a nonplanar five-vacancy cluster (V_5^-), Phys. Rev. B8, 2810 (1973).

5. G.D. Watkins and J.W. Corbett, Defects in irradiated silicon: electron paramagnetic resonance and electron-nuclear double resonance of the Si-E center, Phys. Rev. 134, A1359 (1964).

6. G.D. Watkins and J.W. Corbett, Defects in irradiated silicon: electron paramagnetic resonance of the divacancy, Phys. Rev. 138, A543 (1965).

7. D.L. Griscom, E.J. Freibele, and G.H. Sigel, Jr., Observation and analysis of the primary Si^{29} hyperfine structure of the E' center in noncrystalline SiO$_2$, Solid State Commun. 15, 479 (1974).

8. F.J. Feigl, W.B. Fowler, and K.L. Yip, Oxygen vacancy model for the E' center in SiO$_2$, Solid State Commun. 14, 225 (1974).

9. E.H. Poindexter, J.N. Helbert, B.E. Wagner, and P.J. Caplan, Esr signatures of defects near the Si/SiO$_2$ interface, IEEE Trans. ED-24, 1217 (1977).

10. E.P. EerNisse, Viscous flow of thermal SiO$_2$ Appl. Phys. Letters 30, 290 (1977).

HISA-FM-631-78